A Self-Consistent Mean Field Model of a Starburst Dendrimer: Dense Core vs Dense Shell

David Boris*

Department of Physics and Astronomy, University of Rochester, Rochester, New York 14627

Michael Rubinstein

Department of Chemistry, University of North Carolina, Chapel Hill, North Carolina 27599-3290

Received March 14, 1996; Revised Manuscript Received July 22, 1996[⊗]

ABSTRACT: We examine the equilibrium properties of a starburst dendrimer. A simple Flory theory is developed for the dependence of the radius of gyration of the starburst on its generation. A self-consistent mean field model is solved numerically to verify the Flory theory predictions and elucidate the density profile within the starburst. The density is found to decrease monotonically from the center of the molecule. Structure factors are calculated from the density profiles. Predictions of the model compare favorably with recent experiments and simulations.

I. Introduction

A starburst dendrimer is a regularly branched molecule formed by fully reacting multifunctional monomer units as sketched in Figure 1. Starburst molecules are made either by divergent synthesis, starting from the initiator core and sequentially filling out generations,[1] or by convergent synthesis, growing branched arms first and then attaching them to a core.[2] There has been considerable research on dendrimer synthesis, and there are many reviews in the literature.[3−7]

Dendritic micelles have shown promise in a host of applications including the storage and delivery of dyes,[8] agrochemicals (pesticides, chelators, toxins, etc.),[9] detergents,[10] catalysts, ions, etc.[11] The pharmaceutical industry could attach site-specific receptors and use them as delivery vehicles for bioreactive molecules[12] or as self-contained microreactors acting as synthetic enzyme analogs.[11] Dendrimers have also been synthesized which exhibit a thermotropic nematic liquid crystalline mesophase.[13] In order to better engineer the desired properties into a starburst dendrimer, one must know how its internal density profile is affected by specific chemical characteristics such as the functionality of the branching monomers, the length of spacers between branch points, and their relative flexibility or rigidity. For a number of technological applications, it is crucial to predict the range of parameters for which a starburst has a dense outer shell with a solvent-filled, hollow inner core. For example, this molecular arrangement may mimic the structure of a cell membrane.

Currently there is a controversy in the literature as to whether the simplest case of an uncharged starburst with flexible spacers has a dense or a hollow inner core. In an analytical calculation, de Gennes and Hervet[14] found the density to be minimal at the core and to increase monotonically to the outer edge. However, a numerical simulation of Lescanec and Muthukumar[15] showed a density maximum at the core with a monotonic decrease to the edge. Both a Monte Carlo simulation by Mansfield and Klushin[16] and a molecular dynamics simulation by Murat and Grest[17] showed a density maximum at the core with a monotonic decrease to the edge, except for a slight local minimum at small radial distances for large dendrimers. To help clear up this controversy, we present the results of an equilibrium self-consistent mean field model which is in good agreement with the computer simulations.

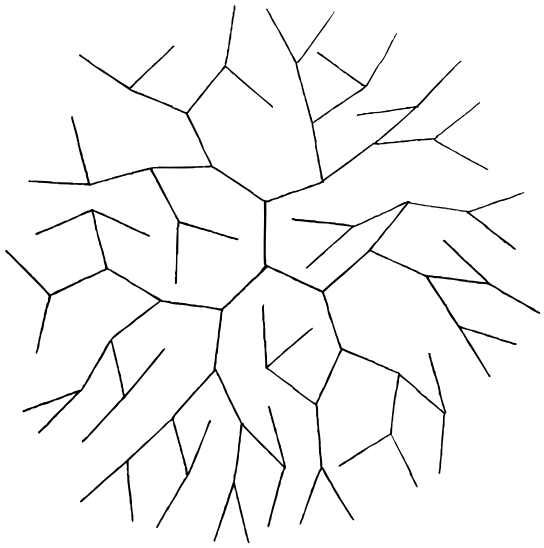

Figure 1. Schematic representation of a trifunctional fifth generation starburst dendrimer.

The first theoretical treatment of the starburst molecule was presented by de Gennes and Hervet.[14] They considered the problem in the limit of long flexible spacers between the trifunctional monomers, in an athermal solvent, with each generation fully reacted. Using a modified version of Edwards' method of self-consistent fields,[18] they derived a density profile which had a minimum at the center of the starburst and increased monotonically to the outer edge.

More recently, Lescanec and Muthukumar[15] performed a three-dimensional, off-lattice numerical simulation of the starburst using a kinetic growth algorithm for a self-avoiding walk. They found the density to be highest at the center and to decrease monotonically to the edge of the molecule. Mansfield and Klushin[19] have shown that the hydrodynamic radii calculated from this kinetic growth model agree well with the experimental data for poly(amido−amine) (PAMAM) dendrimers. In addition, the kinetic growth model[15,19] predicts a maxi-

[⊗] Abstract published in *Advance ACS Abstracts,* September 15, 1996.

S0024-9297(96)00397-X CCC: $12.00

mum in the intrinsic viscosity with increasing molecular weight. This prediction has been verified experimentally,[20] giving some credence to this model despite its nonequilibrium nature. Recently, a Monte Carlo simulation was performed by Mansfield and Klushin[16] on dendrimers of up to nine generations on a diamond lattice. Qualitatively, their results are very similar to Lescanec and Muthukumar's. Contemporaneous with the submission of this paper, a molecular dynamics study by Murat and Grest[17] also gives evidence of a density distribution which is maximal at the core and decays to the edge of the dendrimer. In addition, they investigated the effects of solvent quality, showing the transition to a compact dendrimer. The numerical simulations[15−17,19] each presented evidence that the free ends were distributed throughout the molecule, not exclusively on the surface as de Gennes and Hervet had assumed.

Another recent study determined the average radial size of a dendrimer through a renormalization group calculation.[21] Unfortunately, the density distribution which gives rise to this radial size was not elucidated.

Clearly, the results of the analytical and numerical approaches conflict fundamentally: de Gennes and Hervet[14] predict a density increasing monotonically from the center, while the numerical simulations[15−17,19] predict a decreasing density profile. Both the de Gennes analytical and the Lescanec−Muthukumar numerical models have shortcomings for describing the equilibrium properties of the starburst molecule. Implicit to de Gennes and Hervet's force balance was the assumption that each successive generation was at a further radial distance from the core, so that the free ends would ultimately lie at the outer surface of the molecule.[14,22] Since the mass of each generation is approximately equal to the sum of the masses of all previous generations and each subsequent generation is assumed to be radially further from the center, it is not surprising that they found a monotonically increasing density profile. Lescanec and Muthukumar's simulation[15] did not allow the structures to relax to more entropically favorable configurations. Thus their model is clearly nonequilibrium in nature. In contrast, the Monte Carlo simulation of Mansfield and Klushin[16] should be sampling equilibrium behavior since it appears to have been run sufficiently long to relax the structures to their equilibrium configurations. Likewise, the molecular dynamics simulation of Murat and Grest[17] was shown to converge to very similar radial dimensions even when started in dramatically different initial configurations.

To resolve the controversy between the analytical and numerical results, we have performed an equilibrium self-consistent mean field (SCMF) calculation and derived a simple analytical equation from Flory theory for the dependence of the radius of gyration upon generation. Qualitatively, our results support the findings of the numerical simulations.

In section II, we present a Flory theory of a starburst dendrimer and discuss the limiting behavior of the dendrimer for large and small excluded volume parameters. In addition, we perform a simple rescaling of the Flory theory to describe the effects of flexible spacers. In section III, we describe the formulation of the SCMF model. In section IV, we compare the Flory theory predictions for the radius of gyration to the SCMF results, to Lescanec and Muthukumar's simulation,[15] to Mansfield and Klushin's simulation,[16] to Murat and Grest's simulation[17] and to experimental data[20] on the hydrodynamic radius. In section V, we calculate the structure factors from the SCMF model and compare them with scattering experiments.[23,24] We also offer predictions for the structure factors to be found by small-angle neutron scattering from starbursts with a deuterated final generation. The results are summarized in section VI.

II. Flory Theory of Starburst Dendrimers

Consider a freely jointed starburst molecule of g generations, containing N monomers, of length b (e.g. Figure 1 for $g = 5$). In the absence of excluded volume interactions, the molecule maximizes its entropy, with each linear strand assuming its Gaussian configuration (the monomers are "ghost" monomers and do not interact). The square root of the molecule's mean square radius of gyration is proportional to the size of a typical linear strand of g monomers:

$$R_0 \approx bg^{1/2} \tag{1}$$

($\approx$ means "is proportional to" (up to numerical prefactors)). The density distribution for a Gaussian starburst (without excluded volume interactions) decays monotonically from the center. For a detailed calculation of the pair correlation function for a Gaussian starburst, see Appendix A. The corresponding structure factor $S(q)$ was calculated by Hammouda.[25] The analytic expression for $S(q)$ is provided in Appendix A.

For a starburst of g generations with a nonzero volume v occupied by each monomer, there is a minimum allowable size R_{min} which corresponds to a space-filling, dense dendrimer:

$$vN(g) = \frac{4}{3}\pi R_{min}^3 \tag{2}$$

In a generation g dendrimer, the number of monomers $N(g)$ is

$$N(g) = 1 + \frac{z((z-1)^g - 1)}{z-2} \tag{3}$$

for a dendrimer with z functional branch points. For simplicity, we assume that we are in the good solvent limit so that the excluded volume parameter is equal to the volume v occupied by a monomer. The volume occupied by the starburst $vN(g)$ in a space-filling state grows exponentially with the number of generations g while the maximum accessible volume $(4/3)\pi g^3 b^3$ only increases cubically with the generation. Since the occupied volume grows faster than the accessible volume with increasing generation, there will always be a maximum attainable generation, g_{max}, beyond which the dendrimer is overdense and cannot fit in physical space. Before this generation is reached, in principle there may be a range of generations for which the dendrimer collapses to a dense state with size R_{min}. Combining (2) and (3) and substituting the largest value allowable for the radius (gb), corresponding to the fully stretched state, we find the maximum generation (ignoring logarithmic corrections in g):

$$g_{max} \approx -\frac{\ln(vz/(z-2)b^3)}{\ln(z-1)} \tag{4}$$

As expected, increasing the excluded volume parameter v decreases the maximum attainable generation. For

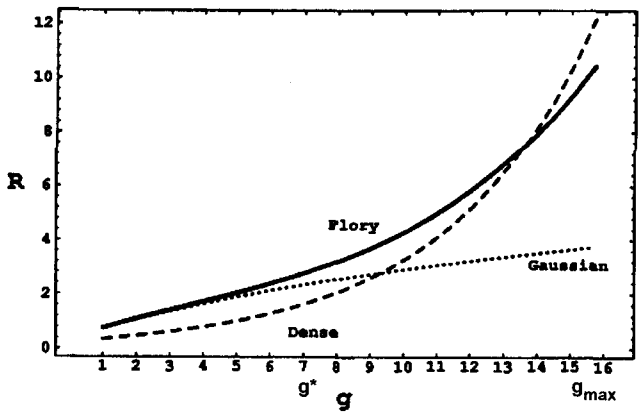

Figure 2. Radius of gyration R_g (in units of b) as a function of generation g. The solid line is the Flory theory prediction for an excluded volume parameter $v' = 0.1b^3$; the dotted line corresponds to the Gaussian state and the dashed line to the dense state (from eq 2: $R_{gmin} = (3/5)^{1/2}R_{min}$). The swelling generation g^* and the maximum possible generation g_{max} are defined in the text.

example, for excluded volume parameter of $v = 0.013b^3$, the maximum possible generation is $g_{max} \approx 15$, while for $v = 0.063b^3$ we find $g_{max} \approx 12$ (these values were chosen because they are in the relevant experimental range). It will be experimentally very difficult to approach the fully reacted generation g_{max}.

If the starburst is not dense, its configuration is determined by balancing the repulsive excluded volume interaction with the entropic energy penalty for swelling the molecule beyond its preferred Gaussian configuration. The Flory[26] free energy for a single linear branch of g monomers in the starburst is

$$\frac{F}{kT} \approx (3/2)\left(\frac{R^2}{R_0{}^2}\right) - 3\ln\left(\frac{R}{R_0}\right) + \frac{vNg}{(4/3)\pi R^3} \qquad (5)$$

The first term gives the entropic contribution to the free energy due to stretching of the branch. The second term is the confinement entropy. The final term is the energy of the excluded volume interaction of a single linear arm of the starburst (with g monomers) with the mean field density due to all the monomers. Minimizing the free energy, we find the equation for the equilibrium size in terms of the linear expansion factor ($\alpha = R/R_0$):[27]

$$\alpha^5 - \alpha^3 = \frac{vNg}{(4/3)\pi R_{0g}{}^3} \approx \frac{vN}{g^{1/2}} \qquad (6)$$

The final scaling form is obtained by substituting for the Gaussian size R_0 its expression from eq 1. The radius of gyration R_g of a dendrimer is proportional to the size R of the typical branch. The solid line in Figure 2 is the radius of gyration R_g of the starburst determined from the Flory theory (solution of eq 6 with an excluded volume parameter of $v = 0.0126b^3$). For small generations ($g < 5$), it is not very different from the Gaussian size (plotted as a dotted line). A starburst with nonzero excluded volume parameter v follows Gaussian statistics if the excluded volume interaction energy is not large enough to cause swelling. We can estimate the generation g^* at which the strand swells to roughly twice its size by equating the mean field approximation of the excluded volume energy in a single linear strand of the starburst to the thermal energy kT:

$$kT\frac{vg^*N(g^*)}{(4/3)\pi R_0{}^3} = kT \qquad (7)$$

For small excluded volume parameter v, corresponding to a large swelling generation g^*, the solution for g^* from eq 7 scales in the same way as g_{max} in eq 4:

$$g^* \approx -\frac{\ln(vz/(z-2)b^3)}{\ln(z-1)} \qquad (8)$$

For example, solving eq 7 numerically, we find that the onset of swelling is at $g^* \approx 4$ for an excluded volume parameter of $v = 0.063b^3$ and that it is at $g^* \approx 7$ for an excluded volume parameter $v = 0.013b^3$ as shown in Figure 2. The behavior of starbursts with less than g^* generations is dominated by the entropic contribution to the free energy. Beyond the g^* generation, the starburst swells as the excluded volume interaction becomes important. The dashed line in Figure 2 is the radius of gyration R_{gmin} of a space-filling state calculated from eq 2. A dendrimer of g generations with this minimum allowable size completely fills its accessible volume like a polymer melt. In Figure 2 for generations larger than 14 the Flory theory predicts an unphysical equilibrium size which is smaller than that of a dense starburst. The Flory theory fails because it neglects the three-body (and higher) excluded volume interactions which are important at these high densities. Since the Flory calculation does not specifically forbid overdense configurations, and the excluded volume energy which acts to swell the starburst is underestimated in this regime, it is not surprising that the resulting equilibrium size predicted is unphysically small. The Flory theory predicts that the dense state is achieved, in general, before the maximum possible generation g_{max}.

We now consider a starburst dendrimer of generation g with flexible spacers. Each spacer consists of s monomers of size b and excluded volume v. The Gaussian size of this dendrimer R_0 is of the order of the size of a linear strand of gs monomers:

$$R_0 \approx b(gs)^{1/2} \qquad (9)$$

We can replace a spacer with s monomers by one with an effective single monomer of size

$$b_{eff} = bs^{1/2} \qquad (10)$$

so that the Gaussian size of the dendrimer is still $R_0 \approx b_{eff}\, g^{1/2}$. The excluded volume parameter of this effective single monomer spacer can be calculated within the mean field approximation. The interaction energy is proportional to kTv times the number of pairwise contacts. Thus the effective excluded volume parameter v_{eff} is equal to the "bare" excluded volume parameter v times the number of monomer pairs s^2 of two interacting "bare" spacers:

$$v_{eff} = vs^2 \qquad (11)$$

We can again use the Flory theory to determine the starburst size by balancing the entropy and the excluded volume interactions. The Flory theory predicts that the dendrimer with flexible spacers has the same size R as the dendrimer with a single monomer spacer of effective size $b_{eff} = bs^{1/2}$ and effective excluded volume parameter $v_{eff} = vs^2$. We will verify this prediction in section IV. Adding flexible spacers provides a means of increasing

the size of the starburst without changing the bare excluded volume parameter. In addition, flexible spacers allow one to make starbursts of larger generations since the mass only increases linearly with the number of monomers in the spacer while the accessible volume increases cubically.

III. Self-Consistent Mean Field Model

In order to investigate more specific details of the density distribution, we performed a self-consistent mean field calculation. Following the ideas of Levine, Thomlinson, and Robinson[28] and Scheutjens and Fleer,[29] we calculated the probability distribution of a single branch of the starburst in the presence of a mean density field due to all of the monomers in the molecule. The mean density field is then recalculated self-consistently by assuming that all branches obey the probability distribution calculated for a single branch. We have incorporated the excluded volume interaction, and the resulting non-Gaussian statistics, entirely through coupling to the self-consistent density field. For the starburst, we exploited the spherical symmetry of the molecule and established a coordinate system with spherical concentric shells of width (b) about the initiator core (of radius $b/2$). To calculate the mean field, we assume that the density is uniformly distributed within the shell. Initially, we assign an average density to each shell, then we use this density profile to calculate the probability distribution for a single branch in this density field. From this probability distribution, we recalculate a new density profile. This process continues until neither changes under repeated iteration and we have found the equilibrium density profile and probability distribution which are the fixed-point solutions.

In the spirit of the recursion relations generated from the matrix method of Di Marzio and Rubin,[30] we calculate the distribution for a test branch of g generations, placed in a mean density field, from a recursion relationship:

$$W_k(j) = q_{j-1,j}W_{k-1}(j-1) + q_{j,j}W_{k-1}(j) + q_{j+1,j}W_{k-1}(j+1) \quad (12)$$

where $W_k(j)$ is the weight for the kth generation of a test branch to be in the jth shell and $q_{i,j}$ is the probability for stepping from shell i to shell j. The weight distribution of the next generation is found from the previous one by multiplying the previous distribution by the probability of making a single step into all accessible shells. Every arm of the starburst starts at the core (the zeroth shell) and makes an initial step into the first shell. This translates into the following initial conditions:

$$W_0(0) = 1; \qquad q_{0,0} = 0; \qquad q_{0,1} = 1 \quad (13)$$

The probability of stepping from the ith shell ($i \geq 1$) into the jth shell is

$$q_{i,j} = f_{i,j}(1 - v'\rho(j)), \quad \text{where} \quad j = \{i - 1, i, i + 1\} \quad (14)$$

with the stepping probabilities normalized such that

$$\sum_{j=i-1}^{i+1} q_{i,j} = 1 \quad (15)$$

The stepping probability $q_{i,j}$ is proportional to the amount of free space available in the jth shell ($1 - v'\rho(j)$), where $\rho(j)$ is the average number density in the jth shell and v' is the excluded volume parameter in the SCMF model. $f_{i,j}$ is a geometrical factor, which slightly favors stepping radially outward since there is more volume in the outer shells. $f_{i,j}$ is given explicitly in Appendix B. The qualitative behavior of the starburst is insensitive to the actual numerical value of the geometric factor $f_{i,j}$.

Starting from the first monomer at the initiator core ($k = 0$), we proceed calculating the weight distribution $W_k(j)$ recursively for each subsequent generation k until the final one is added ($k = g$). The probability for a monomer from the kth generation to be in the jth shell, $P_k(j)$, is determined by normalizing the weight distribution $W_k(j)$:

$$P_k(j) = \frac{W_k(j)}{\sum_{i=0}^{g} W_k(i)} \quad (16)$$

Thus we are able to calculate the probability distributions for each generation of the test branch in the presence of a density profile $\rho(j)$. We close the system of equations self-consistently by calculating a new average density profile from this probability distribution:

$$\rho(j) = \frac{(\sum_{k=0}^{g} N_k P_k(j))}{V(j)} \quad (17)$$

The probability $P_k(j)$ for the kth generation to be in the jth shell multiplied by the number of monomers N_k in that generation gives the contribution to the mass in the jth shell from the kth generation. Summing the contributions from all generations k and dividing by the volume in the shell $V(j)$ gives us the number density $\rho(j)$ in each shell. So, using this method, we can calculate a density profile given the probability distribution. We now enforce self-consistency and generate iteratively the equilibrium (fixed point) probability distribution and density profile.

In this model, we can change the functionality of the branch points, the spacer length, and the excluded volume parameter v'. The model allows us to calculate the overall density profile and the spatial distribution of any generation of interest in the system.

Clearly, this theory has all the inherent assumptions of any mean field theory, since we calculate the excluded volume interaction of a test branch with a mean density field found by preaveraging over configurations of all the other monomers. In particular, we are ignoring all correlations along the branch. To calculate the radius of gyration of the starburst, the mass of the shell is assumed to be uniformly distributed in the shell. In addition, by averaging over angular variables, we assume that the molecule is spherically symmetric with the center of mass at the core monomer which is located at the center of the molecule. For dendrimers with excluded volume interactions, we expect that the approximation of spherical symmetry improves with increasing generation as the dendrimer densifies.

IV. Results

We focus upon trifunctional starbursts ($z = 3$) to compare the predictions of the self-consistent mean field

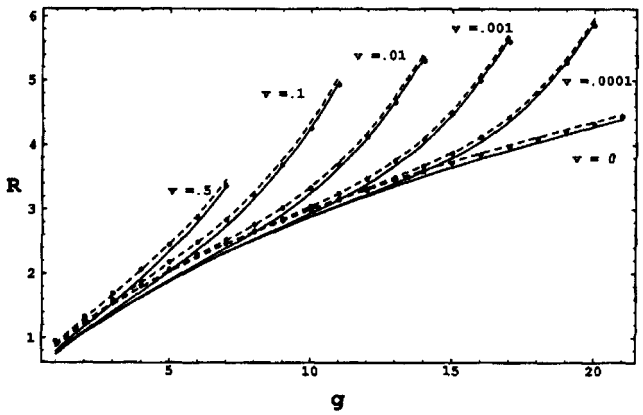

Figure 3. Radius of gyration R_g (in units of b) as a function of generation g. The data points are from the SCMF model for $v' = \{0, 0.0001, 0.001, 0.01, 0.1, \text{and } 0.5 \text{ (units of } b'^3)\}$ from bottom right to upper left, respectively, the lines are from Flory theory with R_{0g} calculated both with respect to the center of the molecule (dashed lines) and with respect to the actual center of mass (solid lines).

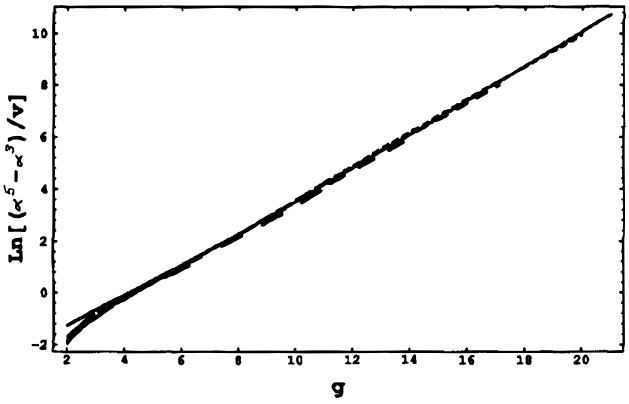

Figure 4. $\ln[(\alpha^5 - \alpha^3)/v]$ as a function of generation g. The Flory theory (solid line) from eq 6 collapses the SCMF model data simultaneously for $v' = \{0, 0.0001, 0.001, 0.01, 0.1, \text{and } 0.5 \text{ (units of } b'^3)\}$ (the overlapping dashed lines).

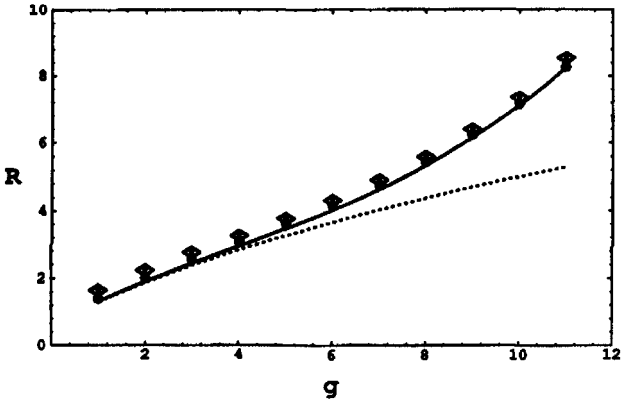

Figure 5. Radii of gyration R_g (in units of b) as a function of generation g for dendrimers calculated from the SCMF theory with $s = 1$; $v' = 0.1(3^{1/2})^3 b'^3$ (diamonds) and for the parameters $s = 3$, $v' = 0.1/3^{1/2} b'^3$ (solid circles) as predicted by the rescaling of the Flory theory. Also shown is the Flory theory for $s = 1$, $v' = 0.1(3^{1/2})^3 b'^3$ (solid line) and for $v' = 0$, $s = 1$ (dotted line).

(SCMF) model and the Flory theory (presented in section II) with numerical simulations[15−17,19] and experiments on PAMAM dendrimers.[20] In Figure 3 we demonstrate the effect of excluded volume interaction on the size R_g of the starbursts. The points are the radii of gyration R_g of starbursts calculated from the SCMF model with a single monomer spacer of scaled step size[31] $b' = 0.92b$ for excluded volume parameters: $v' = 0$, $v' = 10^{-4}$, $v' = 10^{-3}$, $v' = 10^{-2}$, $v' = 10^{-1}$, and $v' = 0.5$ (in units of b'^3) respectively from bottom right to top left in Figure 3. The solid and dashed curves are calculated from the Flory theory using two different approximations for the Gaussian radius of gyration R_0 for a dendrimer with a single monomer spacer of length b and the same set of excluded volume parameters used in the SCMF calculation but rescaled by a single fitting constant $v = 7.9v'$.[32] The lowest pair of curves and set of points show the dependence of radius of gyration R_g on generation number g for Gaussian dendrimers ($v' = 0$). The curves corresponding to finite excluded volume parameters ($v' > 0$) follow the Gaussian dependence for small generations ($g < g^*$) and deviate from it as larger starbursts swell (for $g > g^*$). The crossover g^* between the two regimes shifts to smaller generations with increasing excluded volume parameter as predicted by eq 7. The results of the SCMF calculations (the points in Figure 3) are in excellent agreement with the Flory theory (dashed curves) that calculates the Gaussian size using the approximation made in the SCMF model, that the center of mass is at the core monomer. From this comparison, we see that the Flory theory very slightly underestimates the radius of gyration at small generations. One can attribute this to both the higher relative importance of non-Gaussian statistics for small dendrimers and to the contribution of the central monomer in the SCMF model.[33] The solid curves are the predictions of the Flory theory which, in calculating R_{0g}, allows for fluctuations of the location of the core monomer in the center of mass frame. The agreement between the solid curves and the SCMF theory is good at large generations, but the SCMF model clearly systematically overestimates the radius of gyration, particularly at small generations, because it fixes the center of mass at the core monomer.

The success of the Flory theory is shown even more clearly in Figure 4 because the numerical results of the SCMF calculations are shown to collapse onto a single universal plot of $\ln[(\alpha^5 - \alpha^3)/v']$ as a function of the generation g (see eq 6). The Flory theory prediction for this function, $\ln[Ng/(4/3)\pi R_0^3]$ (plotted as a solid curve) is in excellent agreement with the results of the SCMF calculations (the various dashed curves which overlap with the solid one) for excluded volume parameters of $v' = 0$, $v' = 10^{-4}$, $v' = 10^{-3}$, $v' = 10^{-2}$, $v' = 10^{-1}$, and $v' = 0.5$ (in units of b'^3). The only disagreement is at small generations where the SCMF and Flory theories slightly deviate as we have discussed above.

For dendrimers with flexible spacers, our rescaling predictions (eqs 10 and 11) were verified for a series of effective excluded volume parameters ranging from 0.01 to 0.5 for spacers containing 1, 2, and 3 monomers. For example, in Figure 5 we compare the radii of gyration as a function of generation for dendrimers with spacers of three monomers ($s = 3$), each monomer of size b', with an excluded volume parameter of $v' = 0.1/3^{1/2} b'^3$ (points in Figure 5) and for dendrimers with spacers of a single effective monomer of size $b_{\text{eff}} = 3^{1/2}b'$, with excluded volume parameter $v_{\text{eff}} = 0.1 b_{\text{eff}}^3 = 0.1(3^{1/2})^3 b'^3$ (the diamonds in Figure 5) as calculated by the SCMF theory. The solid line is the Flory theory prediction for the latter set of parameters ($s = 1$, $b_{\text{eff}} = 3^{1/2}b$, $v_{\text{eff}} = 0.1(3^{1/2})^3 b'^3$). The Gaussian case ($s = 1$, $b_{\text{eff}} = 3^{1/2}b$, $v = 0$) is shown as the dotted line. Figure 5 demonstrates that the rescaling theory (eqs 10 and 11) works very well and that the two sets of dendrimers indeed have the same size. The excellent agreement in Figure

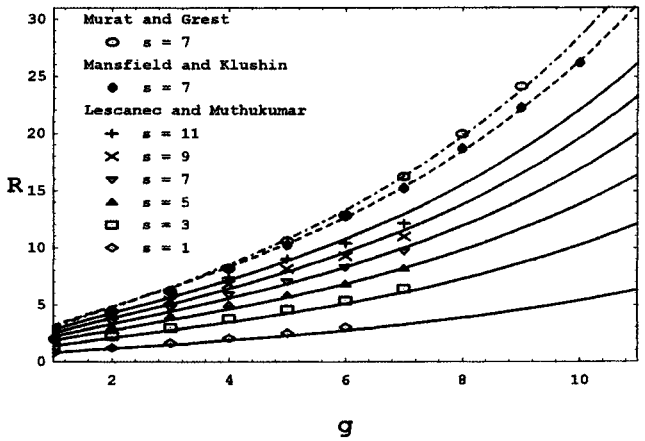

Figure 6. Comparison of the root mean square radii of gyration in units of monomer length b from Lescanec and Muthukumar's simulation[15] (symbols in legend) for 1, 3, 5, 7, 9 and 11 step spacer dendrimers, from Mansfield and Klushin's simulation[16] (solid circles), and from Murat and Grest's simulation[17] (open circles) for 7 step spacer dendrimers with the Flory theory. The Flory prediction for the comparison with Lescanec and Muthukumar's data uses excluded volume parameters predicted by eqs 10 and 11 from a bare single spacer of excluded volume $v' = 0.41b^3$ (solid lines). For comparison with Mansfield and Klushin's data, the Flory theory with effective spacer size $b_{eff} = 3.5b$ and effective excluded volume parameter $v' = 2.3b^3$ (dashed line) is used. The dot−dashed line is the best fit Flory theory to Murat and Grest's data with excluded volume parameter of $v' = 6.56b^3$.

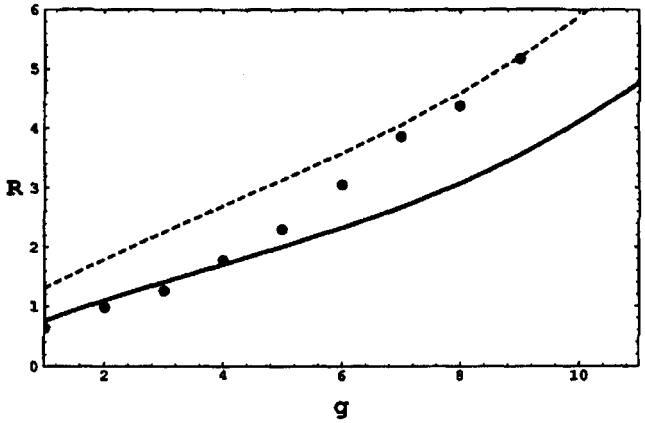

Figure 7. Comparison of experimental hydrodynamic radii (solid circles) with the radii of gyration calculated from Flory theory for $v' = 0.1b'^3$ (solid line) as a function of generation g. The dashed line shows R_{90} calculated from the SCMF model.

5 shows conclusively the validity of the Flory theory for predicting the size of starbursts with flexible spacers.

In Figure 6 we plot the radii of gyration obtained in the numerical kinetic growth simulation of Lescanec and Muthukumar for dendrimers with 1, 3, 5, 7, 9, and 11 step spacers between generations.[15] Lescanec and Muthukumar used a ball and stick model, with bare step size $b = 1.2$ and sphere radius $r = 0.5$, to represent the dendrimer and ensure no overlap between spheres quantitatively. In our model, the excluded volume parameter v measures the total volume which a single monomer renders unavailable to other monomers. We used a least-squares fitting procedure to find the Flory theory excluded volume parameter of $v' = 0.41b^3$ which best fits all of their data sets simultaneously using the scaling relations developed for spacers (eqs 10 and 11). The six solid lines in Figure 6 are the Flory theory curves using this single fit parameter. Over most of the range of the data the fit is quite reasonable. However, the data for 9 and 11 step spacer dendrimers at the sixth and seventh generations systematically fall below the predicted curves. The 1 and 3 step spacer dendrimer size is slightly underpredicted as well. By increasing the excluded volume parameter, we can improve the fit for dendrimers with small spacers (the best fit excluded volume parameter to the single step spacer data ($s = 1$) is $v' = 0.91b^3$) at the expense of the larger spacer ones (or vice versa). While it is possible that the nonequilibrium nature of their simulation is responsible for this discrepancy, it is more likely that the discrepancy is due to our mean field assumption used in rescaling the excluded volume of spacers (see eq 11).

The radii of gyration for dendrimers with seven monomer spacers of step size $b = 3^{1/2}$ between trifunctional junctions were calculated by the Monte Carlo simulation of Mansfield and Klushin[16] (solid circles in Figure 6). In order to compare their results with a rescaled dendrimer with a single monomer spacer, we determine the effective step size $b_{eff} = 3.5b$ so that the end-to-end size of the single step spacer is the same as their seven step spacer. The discrepancy between this value and the one predicted by eq 10 of $b_{eff} = 7^{1/2}b_p$ is due to the increased persistence length $b_p = 1.33b$ for walks on a diamond lattice. The dashed line in Figure 6 is the prediction of the Flory theory for the rescaled dendrimer with a single monomer spacer between generations with step size b_{eff} and a fitted excluded volume parameter of $v' = 2.30b^3$ ($v_{eff} = 2.63b_{eff}^3$). The agreement between the simulation results and the analytical theory (with one adjustable parameter v') is quite good, especially at large generations where the Lescanec and Muthukumar simulation already shows some downward deviation for the same number of spacers ($s = 7$). The excluded volume parameter fit to this simulation is larger than that found for the best fit to all the Lescanec and Muthukumar[15] simulation data ($v' = 0.41b_p^3$). The increased persistence length on the diamond lattice of Mansfield and Klushin[16] and the small size of the excluded volume beads of Lescanec and Muthukumar[15] help explain the difference between the excluded volume parameters measured.

The open circles shown in Figure 6 are the molecular dynamics simulation data of Murat and Grest[17] for dendrimers with seven step spacers ($s = 7$) plotted in units of their average bond length ($b = 0.97\sigma$ in their units) for an athermal dendrimer. The dot-dashed line is the Flory theory with a least-squares fit excluded volume parameter of $v' = 6.56b^3$. This fit excluded volume parameter is larger than that found in fitting the simulation of Mansfield and Klushin[16] for the same number of monomer spacers ($s = 7$) between generations. Most likely, this difference is due to the differences in persistence length and excluded volume (potential shape and size for molecular dynamics) inherent in these simulations.

The experimentally measured hydrodynamic radii (R_h) of PAMAM dendrimers[20] are compared with the radii of gyration (R_g) predicted by the Flory theory. The experimental data for R_h are shown in Figure 7 (solid circles) to follow the Flory theory prediction for R_g with $v' = 0.1b'^3$ (solid line) fairly well at smaller generations ($g < 4$), but for larger generations ($g > 6$), R_h crosses over toward an average value of R_{90} (dashed line), the radius inside of which 90% of the monomers lie, as determined from the SCMF model. This is entirely consistent with the findings of Klushin and Mansfield,[19] who showed that the dependence of R_h upon generation is stronger than that of R_g at generations larger than

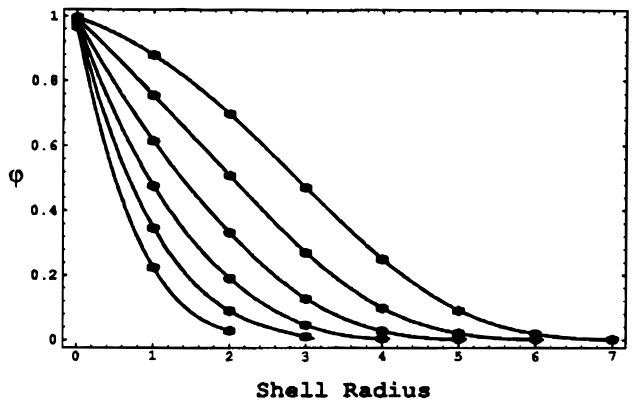

Figure 8. Density profile $\rho(j)$ of starbursts: volume fraction ($\varphi = v\rho(j)$) as a function of radial distance for excluded volume parameter $v' = 0.5b'^3$ for starburst of generation $g = 2-7$.

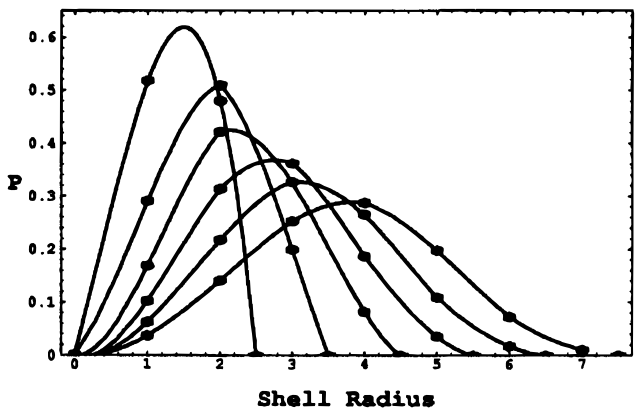

Figure 9. Free end probability distribution as a function of radial distance for excluded volume parameter $v' = 0.5b'^3$ for starbursts of generation $g = 2-7$.

five ($g > 5$). In fact, they gave bounds for R_h that crossed between R_g and R_{90} exactly as we observe. The fitted value of $v' \approx 0.1b'^3$ (where b' is the monomer size) is reasonable for the experimental system because it allows them to be grown beyond the 10th generation (which have been made experimentally) and predicts a dense state somewhere between the 11th and 15th generation. This excluded volume parameter gives reasonable fits to the scattering data as well (see section V, Figure 10, for instance).

As evident from Figure 8, our results support the contention that the density is largest at the core and decays monotonically to the edge. This monotonic profile is seen for all cases studied. This profile is in near-quantitative agreement with the density profiles shown in ref 15 (once volume fraction is converted to density). These profiles are also qualitatively very similar to those found by the Monte Carlo simulation of Mansfield and Klushin.[16] Their data show two features that ours do not. At very small radial distances, on the order of their lattice spacing, they find sharp peaks and valleys in their density due to their lattice approximation. At small radial distances (but larger than their lattice spacing), they find a small local density minimum. Murat and Grest[17] find a similar local minimum in the density distribution at small radial distances. This slight minimum is inconsistent with our results. However, this is the region where their data are least reliable due to poor statistics. Beyond this region the simulation data is smooth and decay monotonically as we would expect, in good agreement with our data.

Chain dynamics studies done through monitoring ^{13}C NMR relaxation of PAMAM dendrimers indicated that the chain dynamics were insensitive to steric crowding that occurs at the molecular surface, but instead showed a gradual slowing of internal chain motion as the molecular weight increases.[34] This is completely consistent with our findings since the molecular crowding does not occur at the surface, instead it is the interior of the dendrimer which begins to sterically crowd with increasing molecular weight (or generation g).

Figure 9 gives direct evidence that the ends are distributed throughout the structure for starbursts of all generations (2nd through 7th generation end probability shown for $v = 0.5b'^3$). Mansfield and Klushin report a similar dependence for 6th generation starbursts with spacers of two monomers[19] ($s = 2$) and with spacers of seven monomers[16] ($s = 7$). The peaks they see at smaller distances are due to the liquid-like short-range ordering in their model. The SCMF model ignores these correlations. The calculated radii of gyration scale proportionally to the position of the peak of the distribution of the final generation (since half of the mass is in this generation). However, it is important to note that approximately one-third of the free ends are distributed inside of this radius. Since the equilibrium position of the last generation is in the interior of the molecule, slow reaction kinetics may limit the experimentally accessible maximum generation (diffusion to the reactive free ends may be greatly sterically hindered).

V. Scattering

The scattering structure factor $S(q)$ measures the amplitude of density correlations on length scales of $2\pi q^{-1}$. Mathematically, $S(q)$ is the Fourier transform of the density−density (two point) correlation function. $S(q)$ is sensitive to both the spatial variations of the average density profile of a system and to correlations between fluctuations of density. We can calculate structure factors from our SCMF density profiles, but, as was noted by Auvrey and de Gennes for the case of adsorbed polymer layers,[35] a mean field approximation loses the correlations between density fluctuations, which are quite important because they contribute a finite fraction to the observed scattering amplitudes at high wavenumbers q. We have devised a straightforward method to reintroduce the scattering from density fluctuations. For Gaussian ($v' = 0$) dendrimers we subtract the scattered intensity due to the mean field density from the analytically known $S(q)$, which was first calculated by Hammouda[25] (the explicit expression is in Appendix A), to obtain the fraction of scattering intensity that is due to fluctuations (I_{gauss}). We simply add this scattering intensity due to Gaussian fluctuations to the scattering intensity due to the mean field density calculated in the SCMF model for finite excluded volume parameters:

$$I_{total} \approx I_{mf} + I_{gauss} \tag{18}$$

Thus we are making a Gaussian approximation for the fluctuations in the system with excluded volume. In general, therefore, we expect to slightly overpredict $S(q)$ since the excluded volume interaction will reduce the magnitude of the density fluctuations.

In Figure 10 we show the Kratky plot for a seventh-generation starburst with a single spacer between generations, $v' = 0.1b'^3$ (solid line) calculated from our

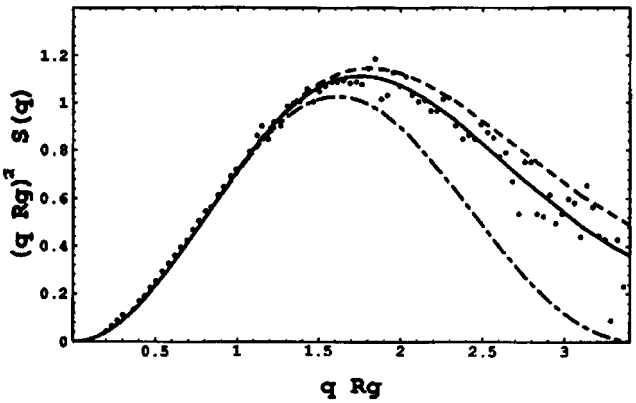

Figure 10. Kratky plot of $(qR_g)^2S(q)$ as a function of qR_g from the analytical calculation with $v' = 0$ (dashed), from the corrected SCMF model with $v' = 0.1b'^3$ (solid), for a solid sphere (dot−dashed), and from experimental data[23] (points) for scattering from a seventh-generation PAMAM starburst.

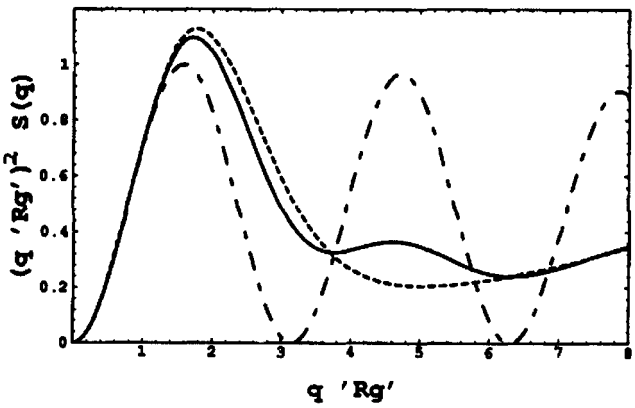

Figure 11. Kratky plot of $(qR_g)^2S(q)$ as a function of qR_g from the SCMF model corrected for Gaussian fluctuations with $v' = 0$ (dashed) and $v' = 0.1b'^3$ (solid) and for a solid shell of width b (dot−dashed) for free ends only of a seventh-generation starburst ("R_g" is calculated from free ends).

SCMF model after adding fluctuation corrections and compare it to experimental data. By plotting $(R_gq)^2S(q)$ vs $q\ R_g$, we remove the length scale dependence and accentuate the differences due to the density distributions. The points are from the SANS experiment on PAMAM dendrimers.[23] As expected, the excluded volume interaction decreases the structure factor from the Gaussian limit shown (dashed curve) because it makes densified regions energetically unfavorable and spreads the density distribution. The structure factor one can calculate from de Gennes and Hervet's predicted density distribution falls slightly below the structure factor for a solid sphere (dot−dashed curve). While there is a large scatter in the data, and our fluctuation correction method introduces an error in our prediction of approximately the same magnitude as the data scatter, the data clearly differentiate between our model and the solid sphere, agreeing well with our predicted structure factor.

Mansfield and Klushin[16] show scattering predictions for 2nd through 8th generation dendrimers with seven step spacers. Qualitatively, we see very similar behavior for $0 < qR_g < 3.5$; however they see a more pronounced secondary maxima at $qR_g \approx 5$ for generations 4−8. For larger q, they see the crossover to the asymptotic behavior caused by fluctuations inside of their self-avoiding correlation blobs. Since the asymptotic behavior is due to self-avoiding correlations, it is missing in our mean field model.

Various predictions for the Kratky plot for a starburst with a deuterated final generation are shown in Figure 11. $S(q)$ and "R_g" are calculated from the density distribution of the last generation only. After correcting for fluctuations using the gaussian results for ends only (the analytical expression for the structure factor is given in Appendix A), the Kratky plot $(S(q)\ (q\text{"}R_g\text{"})^2)$ predicted by the SCMF model with $v' = 0.1b'^3$ (solid curve) shows a pronounced secondary maxima not present in the Gaussian (dashed) curve. Also shown is the corresponding Kratky plot for the spherical shell assumed by de Gennes and Hervet (dot−dashed line). We hope forthcoming experiments will be able to distinguish between these predictions because of the large difference in the height of the secondary maxima.

VI. Conclusions

Our principal findings are as follows: (i) Our self-consistent mean field model conclusively shows that flexible dendrimers have dense, not hollow, cores. (ii) For all cases studied, the density is greatest at the core and decays to the edge of the dendrimer, in agreement with the various numerical simulations[15−17,19] in the literature. (iii) Our simple Flory theory incorporates the basic physics and predicts the size of the starburst. (iv) We have derived and verified expressions for the rescaling of the excluded volume parameter and step size caused by the addition of a spacer consisting of a flexible chain of monomers between trifunctional junction points. (v) The addition of flexible spacers spreads the density distribution to further radial distances and allows starbursts of larger generations to be made by reducing the effective excluded volume parameter in the Flory theory in a predictable, controllable way. (vi) The experimental hydrodynamic radii for PAMAM dendrimers follow the qualitatively expected behavior crossing between our predictions for R_g and R_{90}. (vii) Our predictions agree well with the experimentally measured structure factor for seventh-generation PAMAM dendrimers. (viii) In direct conflict with the assumption of de Gennes and Hervet, but in agreement with all of the computer simulations, we find that the ends are distributed throughout the volume of the dendrimer.

It is easy to understand the basic physics controlling the density distribution of the starburst dendrimer. A starburst determines its configuration by balancing the repulsive monomer−monomer excluded volume interaction with the entropic energy penalty for swelling the molecule beyond its preferred Gaussian configuration. The excluded volume parameter v controls the crossover between the two limiting cases in which either entropy or the excluded volume interaction dominates. In the Gaussian limit ($v = 0$), entropy dominates and we have shown that the dendrimer's equilibrium density profile has a density maximum at the core and decays monotonically with increasing radius. As the system approaches the dense limit the excluded volume interaction dominates, driving the system toward a uniformly dense state. Since the configuration of the starburst is determined by the balance of two forces, due to entropy and the excluded volume interaction, neither of which prefer a hollow core, it is not surprising that for all cases studied the density is greatest at the core and decays monotonically to the edge.

In the future, it may be useful to include more advanced structural and spatial correlations in a self-consistent mean field model. This is particularly motivated by a second Monte Carlo simulation of Mansfield

which shows that dendrons (branches) within a dendrimer segregate despite being chemically identical.[36] Murat and Grest[17] further quantified dendron segregation, showing that larger dendrons (high-generation dendrimers) segregate more completely. Dendron segregation is an entirely expected phenomenon since the criteria for monodisperse branched polymers to overlap is simply that the Gaussian dimension of the polymer is less than the spatial dimension. Since starburst dendrimers have an infinite Gaussian dimension but are confined to exist in three-dimensional space, they cannot overlap and should segregate. Our current mean field model does not contain the structural correlations nor does it retain the angular spatial information needed to describe dendron segregation. We do not expect dendron segregation to have a major effect upon the mean density distributions and radii of gyration of dendrimers as can be seen by the good agreement of our model with both experiments and simulations.

Since many of the technological applications for starbursts require a hollow interior, it is important to point out that such a structure can be engineered. If the branches of the starburst were very rigid, so that the persistence length of a test branch were greater than its contour length, then each successive generation would be at a further radial distance and a relatively hollow interior would result. Other methods to control the structure include using charges, chemical segregation effects, or flexible spacers (the number of which may be generation dependent). Specifically, one could envision using a very rigid polymer for the first 5−8 generations and then attaching a much more flexible polymer for the final few generations. The flexible polymer would form a dense outer shell, and as long as the flexible ends could not reach all the way back to the center, the resulting molecule would be relatively hollow. If these ends were charged they could be induced to change configuration based upon the salt concentration (screening), selectively closing or opening the surface of the starburst. Clearly, this is only speculation, but the important point is that our results do not preclude such engineering, instead they point the proper direction for further research.

Acknowledgment is made to the donors of the Petroleum Research Fund, administered by the American Chemical Society, for support of this research.

Appendix A

In this appendix we give the analytical function n_L for the number of distinct pairs of monomers separated by a distance L along the backbone of the dendrimer. Then we use this function to calculate the radius of gyration R_g and the structure factor $S(q)$. For a trifunctional gaussian starburst dendrimer of generation g, one can obtain:

$$n_L = \begin{cases} 3 \times 2^{L-1}(3 \times 2^{g-(L/2)-1} - 1); & L \text{ even, } L \le 2g-2 \\ 3 \times 2^{L-1}(2^{g-((L-1)/2)} - 1); & L \text{ odd, } L < 2g-2 \\ 3 \times 2^{2g-2}; & L > 2g-2 \end{cases} \quad \text{(A1)}$$

Using this result, one can calculate the radius of gyration:

$$R_g^{\,2} = \sum_{L=0}^{2g} n_L L b^2/N^2 \quad \text{(A2)}$$

which equals

$$R_g^{\,2} = 3b^2\frac{(-1 + 6 \times 2^g + (3g-5)2^{2g})}{(3 \times 2^g - 2)^2} \quad \text{(A3)}$$

For large-generation Gaussian dendrimers ($g \gg 1$), the radius of gyration is $R_g^2 \approx gb^2$ (See eq 1). The scattering function $S(q)$ is found by summing the contributions from the Gaussian distribution for each strand n_L:

$$S(q) = \frac{2}{N(N-1)}\sum_{L=0}^{2g} n_L e^{-q^2b^2L/6} \quad \text{(A4)}$$

After a straightforward calculation, we find

$$S[x] = 6e^{-x/3}[-2 + 3 \times 2^{g-1} - e^{x/6} + 4e^{-x/3} + 2e^{-x/6} + 2g(e^{x/6} - 6e^{-x/3} - 4e^{-x/6}) + 2^{2g-2}e^{x(g-1)/3}(2e^{-x/3} + 8e^{-x/2} + 8e^{-2x/3})]/(3 \times 2^g - 2)(3 \times 2^g - 3) \times (1 - 2e^{-x/3})(1 - 4e^{-x/3})$$

where $x = q^2b^2$.

Similarly, we may calculate the "R_g" and $S(q)$ from just the free ends using the same method. First we obtain the number of distinct pairs n_L which contain only free ends separated by a distance L:

$$n_L = \begin{cases} 3 \times 2^{g+(L/2)-3}; & L \text{ even, } L < 2g \\ 0; & L \text{ odd} \\ 3 \times 2^{2g-2}; & L = 2g \end{cases} \quad \text{(A5)}$$

Now using eq A2, we solve for the effective radius of gyration for end monomers only:

$$R^2_{\text{ends}} = \frac{1}{3}[2^{1-g} - 2 + 3g]b^2 \quad \text{(A6)}$$

For large Gaussian starbursts ($g \gg 1$), we find $R_{\text{ends}}^2 \approx R_g^2 \approx gb^2$. The structure factor for scattering from only the last generation monomers of a Gaussian starburst can be attained by substituting eq A5 into eq A4. This calculation yields

$$S[x] = \frac{[1 - e^{x/3} + 2^{g-1}e^{-xg/3} + 2^{g+1}e^{-x(g+1)/3}]}{(3 \times 2^{g-1})(1 - 2e^{-x/3})} \quad \text{(A7)}$$

This analytical expression for the structure factor from scattering due to the end monomers is the dashed line plotted in Figure 11.

Appendix B

Below we calculate the probability f_{kj} that a randomly oriented step of size b with one end at an arbitrary point in shell k has the other end in shell j. This probability f_{kj} is a geometrical factor influencing the probability q_{kj} of stepping from shell k to j (eq 14). It is calculated by finding the percentage of the surface area of a sphere of radius $r = b$ centered on all possible coordinates in adjacent shell k which falls in shell j. The spherical surface represents the possible positions of the ends of a random step of length b with uniform distribution of orientations. We obtain

$$f_{k,k-1} = \frac{1}{4}\left(-k + 2 + \left(k^2 - k - \frac{3}{4}\right)\ln\left[\frac{(2k+1)}{(2k-1)}\right]\right)$$

$$f_{k,k} = \frac{1}{2}k\ln\left[\frac{(2k+1)}{(2k-1)}\right] \qquad \text{(B1)}$$

$$f_{k,k+1} = \frac{1}{4}\left(k + 2 + \left(-k^2 - k + \frac{3}{4}\right)\ln\left[\frac{(2k+1)}{(2k-1)}\right]\right)$$

References and Notes

(1) Tomalia, D. A.; Baker, H.; Dewald, J.; Hall, M.; Martin, S.; Roeck, J.; Ryder, J.; Smith, P. *Polym. J.* **1985**, *17*, 117.
(2) Hawker, C. J.; Frechet, J. M. J. *J. Chem. Soc., Chem. Commun.* **1990**, *15*, 1010.
(3) Newkombe, G. R.; Moorefield, C. N.; Baker, G. R. *Aldrichim. Acta* **1992**, *25* (2), 31−8.
(4) Engel, R. *Polym. News* **1992**, *17* (10), 301−5.
(5) Kakimoto, M.; Morikawa, A. *Shinsozai* **1994**, *5* (8), 75−81 (Japanese).
(6) Li, Y. *Gaofensi Tongbao* **1993** (3), 155−64 (Chinese).
(7) Dagani, R. *Chem. Eng. News* **1996**, *74* (23), 30.
(8) Winnik, F. M.; Davidson, A. R.; Breton, M. P. U.S. Patents 92-964802, 91-646904, 91-722441 (Xerox Corp.).
(9) Tomalia, D. A.; Wilson, L. R. U.S. Patent 86-897455 (Dow Chemical Co.).
(10) Newkombe, G. R.; Moorefield, C. N. U.S. Patent 91-657683 (University of South Florida).
(11) Tomalia, D. A.; Naylor, A. M.; Goddard, W. A., III *Angew. Chem., Int. Ed. Engl.* **1990**, *29*, 138.
(12) Szoka, F. C., Jr.; Haensler, J. U.S. Patent 93-92200 (University of California).
(13) Percec, V.; Kawasumi, M. *Macromolecules* **1992**, *25* (15), 3843.
(14) de Gennes, P.-G.; Hervet, H. *J. Phys. (Paris)* **1983**, *44*, L351.
(15) Lescanec, R. L.; Muthukumar, M. *Macromolecules* **1990**, *23*, 2280.
(16) Mansfield, M. L.; Klushin, L. I. *Macromolecules* **1993**, *26*, 4262.
(17) Murat, M.; Grest, G. S. *Macromolecules* **1996**, *29*, 1278.
(18) Edwards, S. F. *Proc. Phys. Soc. London* **1965**, *85*, 613.
(19) Mansfield, M. L.; Klushin, L. I. *J. Phys. Chem.* **1992**, *96*, 3994.
(20) Mourey, T. H.; Turner, S. R.; Rubinstein, M.; Frechet, J. M. J.; Hawker, C. J.; Wooley, K. L. *Macromolecules* **1992**, *25*, 2401.
(21) Biswas, P.; Cherayll, J. *J. Chem. Phys.* **1994**, *100* (4), 3201−9.
(22) Mansfield, M. *Chemtracts—Macromol. Chem.* **1991**, *2*, 364.
(23) Bauer, B. J.; Briber, R. M.; Hammouda, B.; Tomalia, D. *ACS PMSE Proc.* **1992**, *66*.
(24) Briber, R. M.; Bauer, B. J.; Hammouda, B.; Tomalia, D. *ACS PMSE Proc.* **1992**, *67*.
(25) Hammouda, B. *J. Polym. Sci., Part B: Polym. Phys.* **1992**, *30*, 1387.
(26) Flory, P. J. *Principles of Polymer Chemistry*; Cornell University Press: Ithaca, NY, 153; p 600.
(27) Doi, M.; Edwards, S. F. *The Theory of Polymer Dynamics*; Oxford University Press: Oxford, 1986; p 30.
(28) Levine, S.; Thomlinson, M. M.; Robinson, K. *Discuss. Faraday Soc.* **1978**, *65*, 202.
(29) Scheutjens, J. M. H. M.; Fleer, G. J. *J. Phys. Chem.* **1979**, *83*, 1619.
(30) Di Marzio, E. A.; Rubin, R. J. *J. Chem. Phys.* **1971**, *55*, 4318.
(31) A rescaled step size of $b' = 0.92b$ was found to correct the SCMF radii of gyration so they agree asymptotically with the analytically calculated radius of gyration for Gaussian dendrimers of step size b. The source of this discrepancy is the assumption of a uniform density distribution within each shell which was used in calculating the probability of stepping between shells.
(32) The SCMF model is a more advanced mean field approximation than the Flory theory since it allows radial density variations which affect the quantitative comparison of the excluded volume parameter in the two models, but remarkably do not affect the qualitative behavior.
(33) The SCMF model places the mass of the monomers at the junctions. Thus the mass of the central monomer is included in the mean field density of the central shell which contributes to the radius of gyration. In the Flory theory calculation, the central mass is assumed to be pointlike, and thus it does not contribute to the radius of gyration around the center of the starburst. This accounts for approximately half of the discrepancy between the SCMF and the Flory theory at small generations.
(34) Meltzer, A. D.; Tirrell, D. A.; Jones, A. A.; Inglefield, P. T.; Hedstrand, D. M.; Tomalia, D. A. *Macromolecules* **1992**, *25* (18), 4541−8.
(35) Auvrey, L.; de Gennes, P.-G. *Europhys. Lett.* **1986**, *2*, 647.
(36) Mansfield, M. *Polymer* **1994**, *35* (9), 1827−30.

MA960397K